Spectral Line Merging in Hydrogen-like Species for Diagnostic of Laboratory and Space Plasmas

E. Stambulchik[1], K. Dzierżęga[2], F. Sobczuk[2], and B. Pokrzywka[3]

[1]Weizmann Institute of Science, Rehovot 7610001, Israel
[2]Jagiellonian University, ul. Łojasiewicza 11, 30-348 Kraków, Poland
[3]Pedagogical University, ul. Podchorążych 2, 30-084 Kraków, Poland

13th Serbian Conference on Spectral Line Shapes in Astrophysics
Belgrade, Serbia
August 23–27, 2021

Introduction

- Plasma density effects result in complex atomic phenomena, including spectral line broadening and delocalization of higher excited levels.
- The resulting ionization potential depression and line merging manifest themselves spectroscopically via “disappearance” of discrete spectral lines.

Various approaches to this problem

E.g., see [Dappen et al., 1987, Rogers and Iglesias, 1992, Tremblay and Bergeron, 2009, D’yachkov, 2016, Lin et al., 2017, Alexiou et al., 2018, Koubiti and Sheeba, 2019].

A comprehensive approach should accurately model the entire spectrum of a spectroscopic series, i.e., the shapes of the individual discrete lines and a smooth transition to the free–bound continuum, preserving the oscillator strength density.

Line merging :: an example

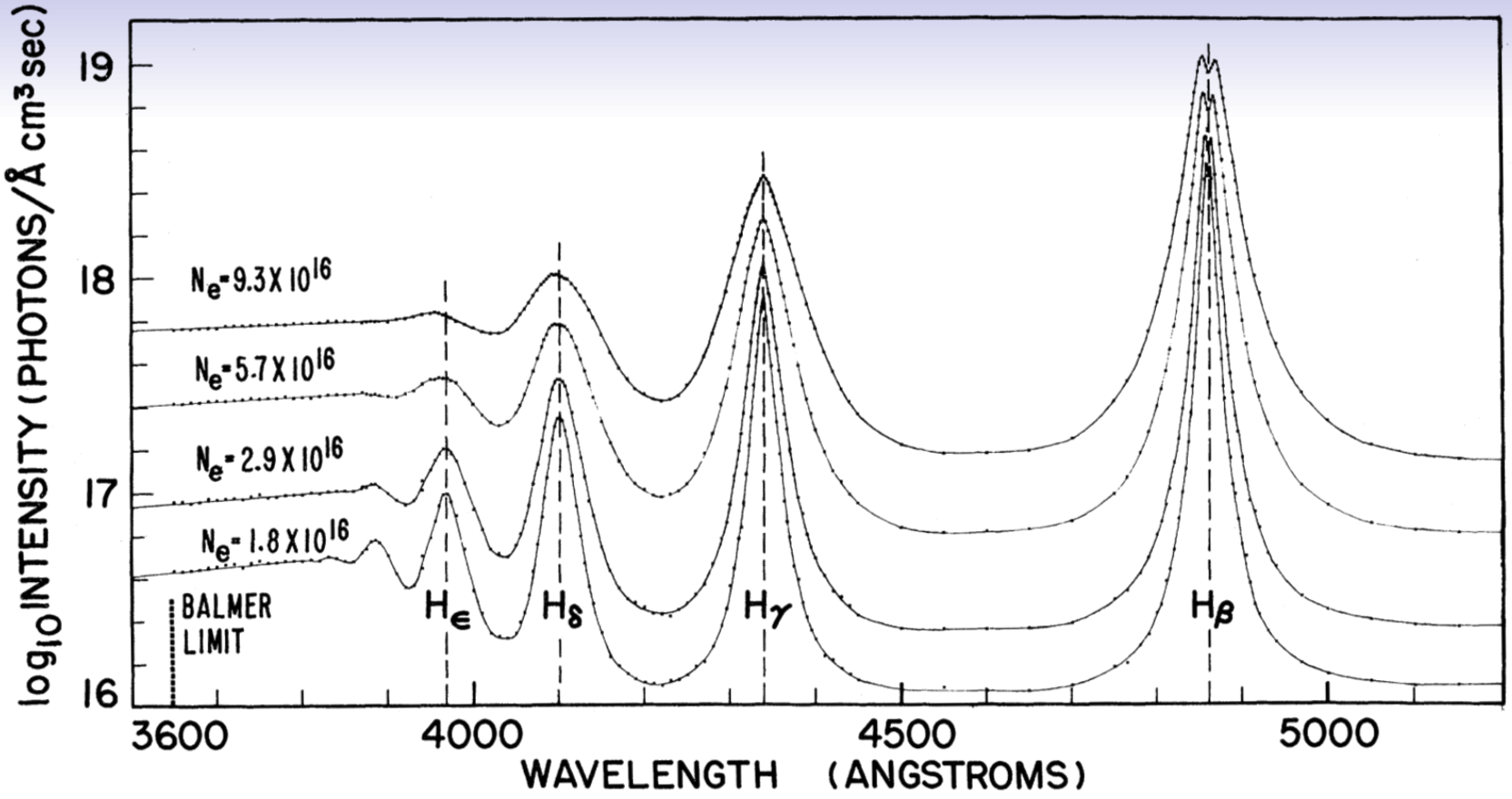

Wall-stabilized arc [Wiese et al., 1972]. The last observed discrete line is clearly a function of the plasma density.

Line merging :: astrophysical examples

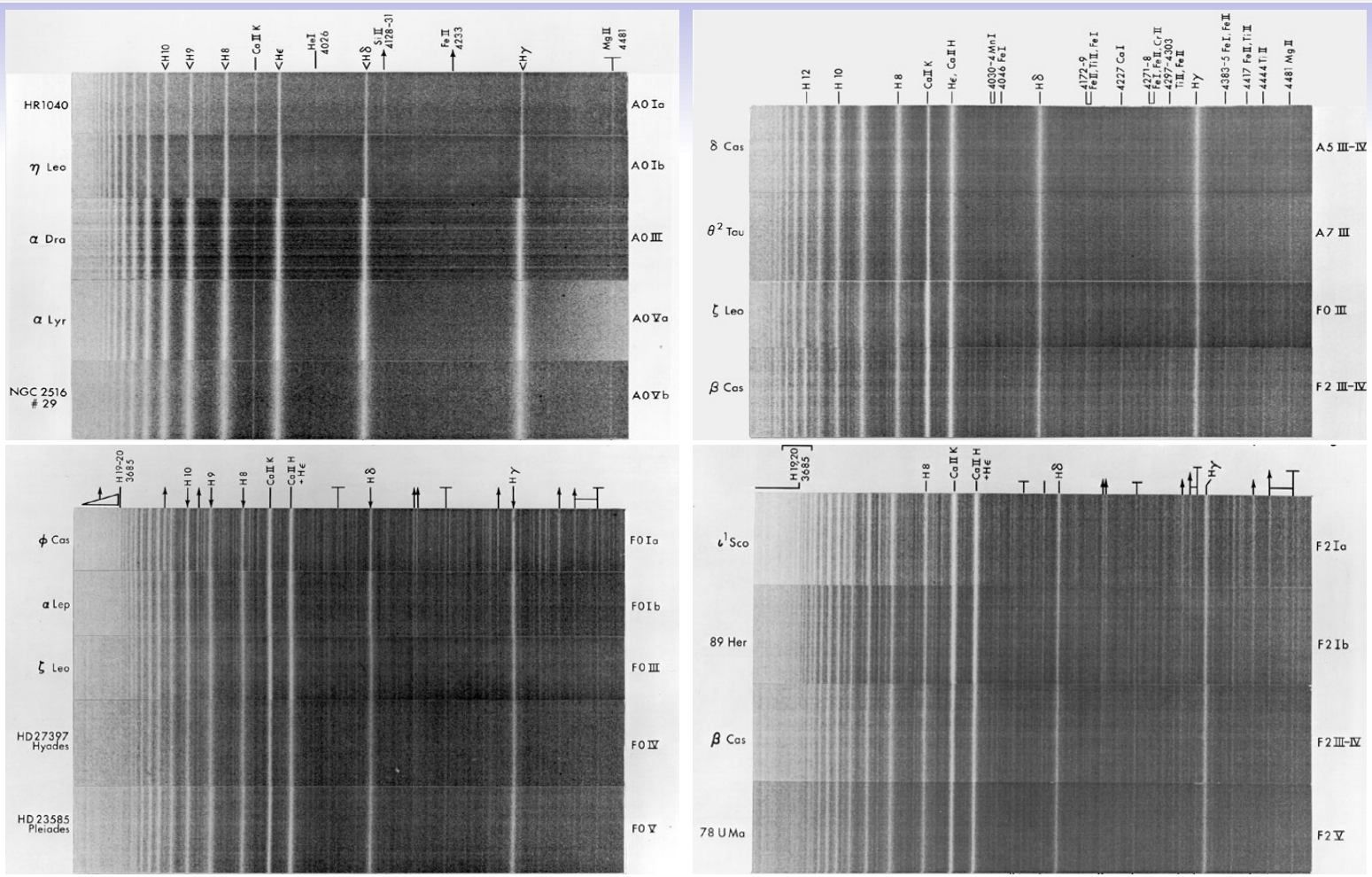

Spectra of various star types [Morgan et al., 1978]. Note the Balmer series merging into the recombination continuum.

High-n transitions

High-n (Rydberg) transitions are challenging for lineshape calculations:

- Number of states $\Rightarrow$ matrix dimension $\sim n^2$
- Computational time $\sim n^6$
- Especially prohibiting for simulations

A fast yet accurate approach is needed.

Quasi-contiguous (QC) approximation :: static shape

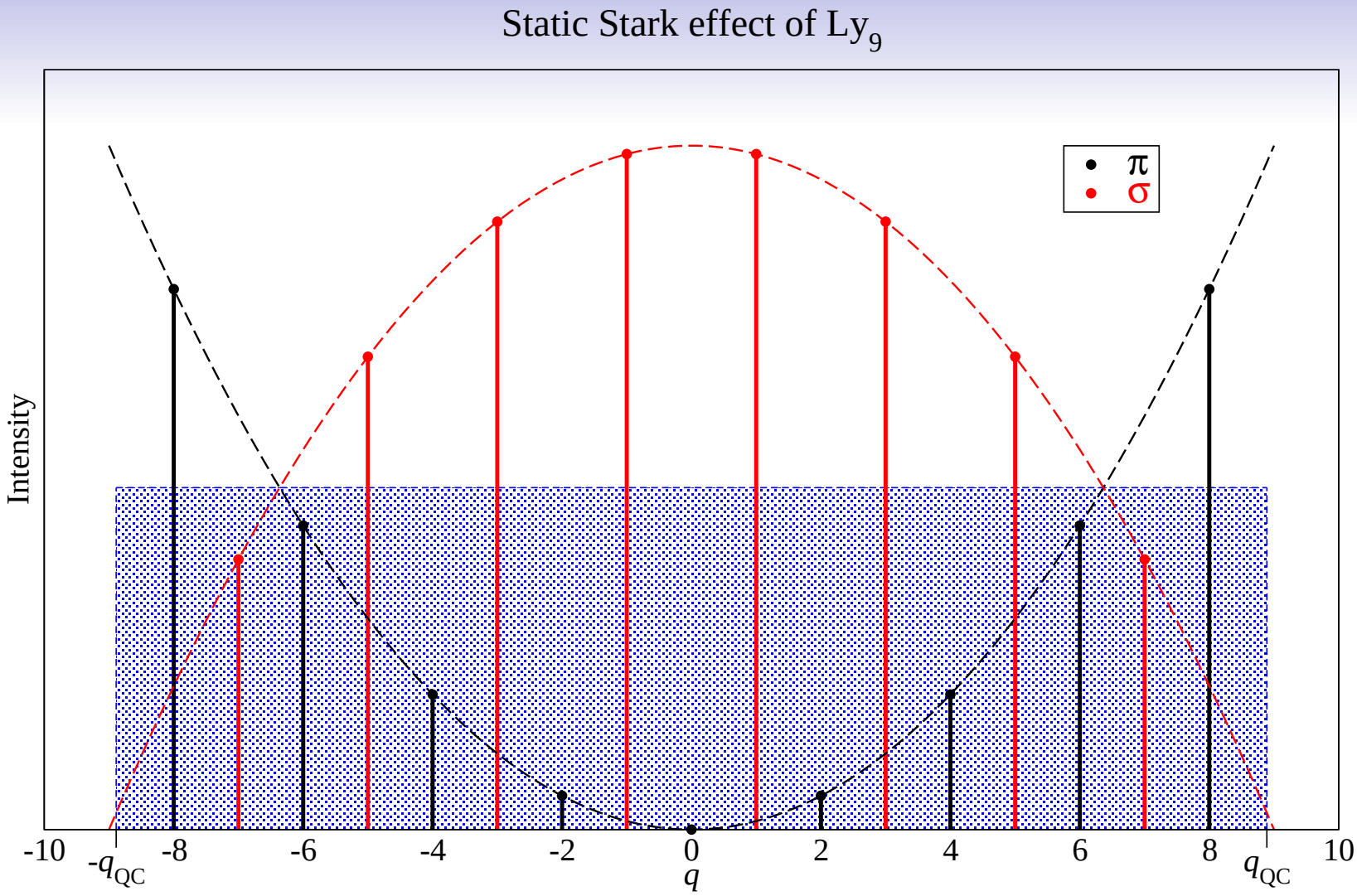

Intensities of the π and σ components form two parabolae, which, on average, can be substituted with a simple rectangular shape.

QC approximation :: quasistatic shape

Apply a microfield distribution $W(F)$:

$$I(\omega) = I^{(0)}_{nn'} \int_{\hbar\omega/\alpha_n}^{\infty} \frac{W(F)dF}{2\alpha_{nn'}F/\hbar} \equiv I^{(0)}_{nn'} L_{\rm qs}(\omega)\,,$$

where $\alpha_{nn'} = \frac{3ea_0}{2Z}(n^2 - n'^2)$ is the static-Stark-effect coefficient.

With the reduced detuning $\bar{\omega} = \omega/\Delta_0$, $\Delta_0 \equiv \frac{\alpha_{nn'}F_0}{\hbar}$, we obtain for ideal plasma:

$$L_{\rm qs}(\bar{\omega}) = \frac{1}{\pi}\int_0^{\infty} \cos(\bar{\omega}x)\exp(-x^{3/2})\mathrm{d}x.$$

[Stambulchik and Maron, 2008]; also corrections due to plasma non-ideality.

Frequency-fluctuation model (FFM)
[Talin et al., 1995, Calisti et al., 2010, Bureeva et al., 2010]
postulates that field fluctuations cause a “diffusion” of the quasistatic intensity distribution with a typical frequency

$$\nu = \frac{\langle v \rangle}{\langle r \rangle} = \sqrt{\frac{kT}{m_p^*}} \left(\frac{4\pi N_p}{3} \right)^{1/3} .$$

Instead of the quasistatic lineshape $L_{\mathrm{qs}}(\bar{\omega})$, the dynamic one is

$$L(\bar{\nu};\bar{\omega}) = \frac{1}{\pi} \Re \frac{J(\bar{\nu};\bar{\omega})}{1 - \bar{\nu} J(\bar{\nu};\bar{\omega})} ,$$

where

$$J(\bar{\nu};\bar{\omega}) = \int \frac{L_{\mathrm{qs}}(\bar{\omega}')\mathrm{d}\bar{\omega}'}{\bar{\nu} + i(\bar{\omega} - \bar{\omega}')} , \quad \bar{\nu} \equiv \nu/\Delta_0 .$$

QC-FFM

Applying FFM to quasi-contiguous lineshape, for ideal one-component plasma one gets:

$$L(\bar{\nu};\bar{\omega}) = \frac{1}{\pi}\Re\frac{J(\bar{\nu};\bar{\omega})}{1-\bar{\nu}J(\bar{\nu};\bar{\omega})}\ ,$$

where

$$J(\bar{\nu};\bar{\omega}) = \int_0^\infty \mathrm{d}\tau \exp\left[-\tau^{3/2} - i(\bar{\omega} - i\bar{\nu})\tau\right]\ .$$

A universal expression, the computation time independent of n, n'. Moreover, the larger $n - n'$, the better accuracy.

[Stambulchik and Maron, 2013]; straightforward extension for multi-component non-ideal plasmas.

QC-FFM :: line merging

The approach (closely following [Griem, 1997]):

- Calculate bound–bound (BB) $n_\ell \to n_u$ shapes for a series of n_u until FWHM exceeds $\left|E_{n_u} - E_{n_u+1}\right|$ (the "Inglis–Teller" reasoning [Inglis and Teller, 1939]) $\Rightarrow$ the last discrete n_m;
- Assume the free–bound (FB) begins at $\left(E_{n_m} + E_{n_m+1}\right)/2$;
- Convolve the FB continuum with the last ($n_\ell \to n_m$) BB lineshape;
- Sum up.

The oscillator strength density is preserved

QC-FFM :: line merging

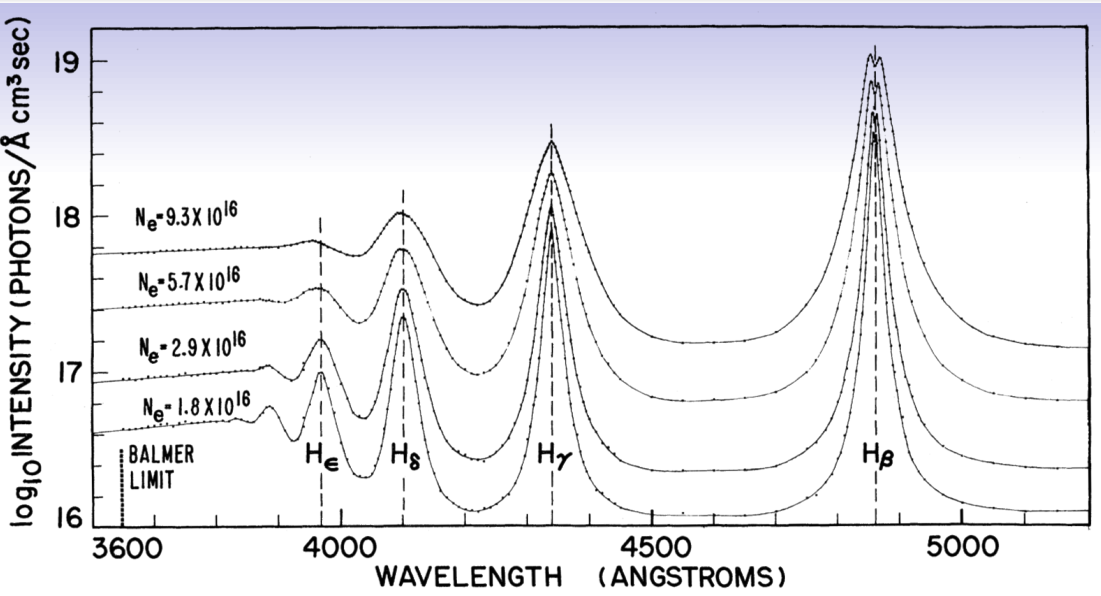

[Wiese et al., 1972]

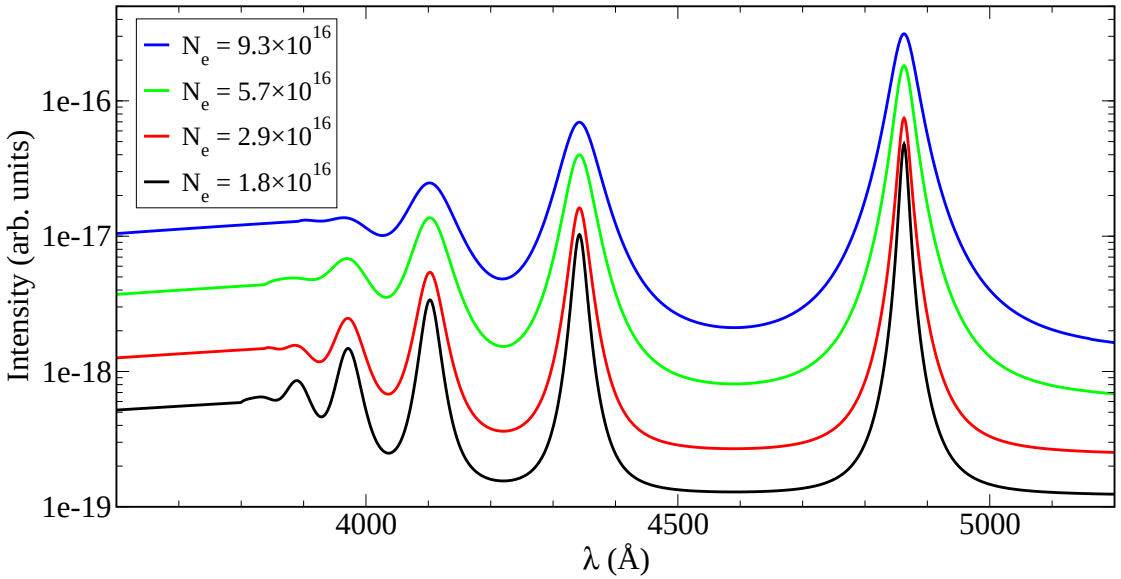

$< 1\,\mathrm{s}$ CPU time

New experiments

The benchmark data [Wiese et al., 1972] are half a century old...

Interested in new experiments that would

- Extend to higher densities;
- Use direct diagnostics of plasma n_e, T_e;
- Also measure T_i.

Thomson scattering (TS) for accurate plasma diagnostics.

Thomson scattering

The power scattered by plasma as a function of $\omega \equiv \omega_s - \omega_L$ is

$$\frac{dP_T(\omega)}{d\Omega}\, d\omega \;\propto\; \frac{d\sigma_T}{d\Omega} S_T(k,\omega)\, d\omega\,,$$

where $d\sigma_T/d\Omega = r_e^2(1-\sin^2\theta\cos^2\varphi)$ is the free-electron TS cross-section and $S_T(k,\omega)$ is the total spectral density function:

$$\begin{aligned} S_T(k,\omega)\, d\omega &= S_e(k,\omega)\, d\omega + S_i(k,\omega)\, d\omega \\ &\approx \left|\frac{1}{1+\alpha^2 W(x_e)}\right|^2 \frac{\exp(-x_e^2)}{\sqrt{\pi}} dx_e \\ &+ Z\alpha^4 \left|\frac{1}{1+\alpha^2+\alpha^2 Z T_e/T_i W(x_i)}\right|^2 \frac{\exp(-x_i^2)}{\sqrt{\pi}} dx_i\,. \end{aligned}$$

Here, $\alpha = (k\lambda_D)^{-1}$, $x_{e,i} = \omega/(kv_{e,i})$, $v_{e,i}$ the electron (ion) thermal velocity, Z the ion charge, λ_D the Debye length, $W(x)$ the plasma dispersion function [Salpeter, 1960, Evans and Katzenstein, 1969].

Thomson scattering

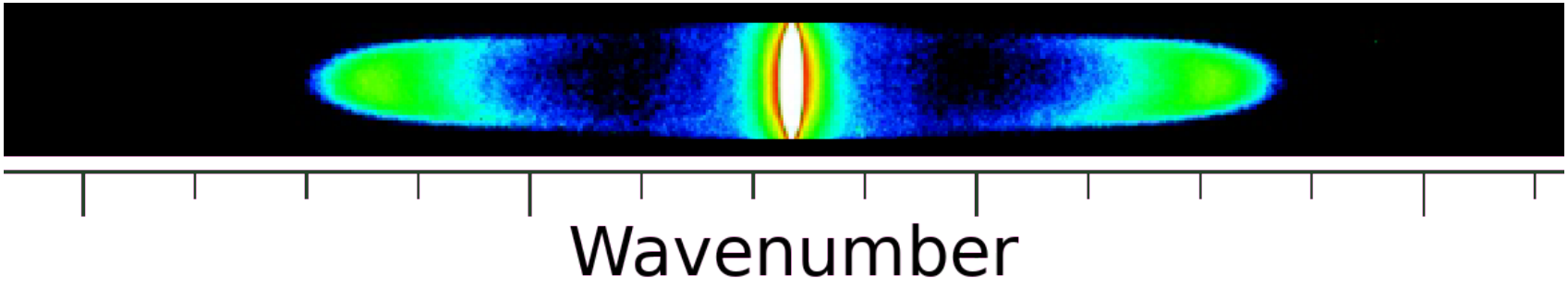

The ion component

- is narrow, occurs in the central part of the scattering spectrum, and so is easily separable;
- depends on the T_e/T_i ratio and can be used to measure the ion temperature provided N_e and T_e are already known.

2-color Thomson scattering

A major experimental challenge

However, the ion component overlaps with the Rayleigh scattering (RS) signal, which inherently accompanies TS in partially ionized plasmas.

To separate the TS and RS contributions, and then to determine T_i, applied was the 2-color Thomson scattering (2CTS) method using two probe lasers of significantly different wavelengths and leveraging the different wavelength dependences of RS and TS [Sobczuk et al., 2021].

Experimental setup

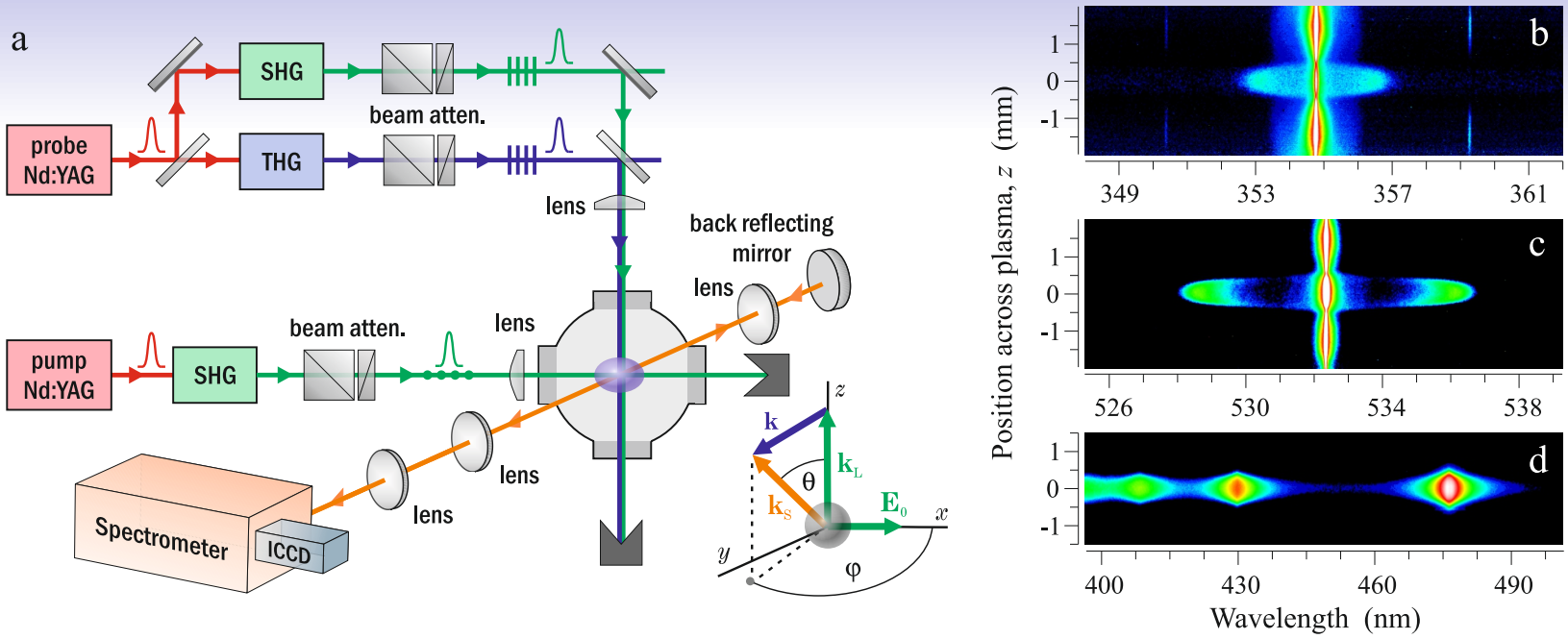

Experimental setup (a) and typical images of TS spectra at $355\,\mathrm{nm}$ (b) and $532\,\mathrm{nm}$ (c) and of plasma emission spectra (d). [Dzierżęga et al., 2021]

The emission and TS spectra were averaged over 10,000 and 50,000 laser shots, respectively.

2CTS analysis :: electron component

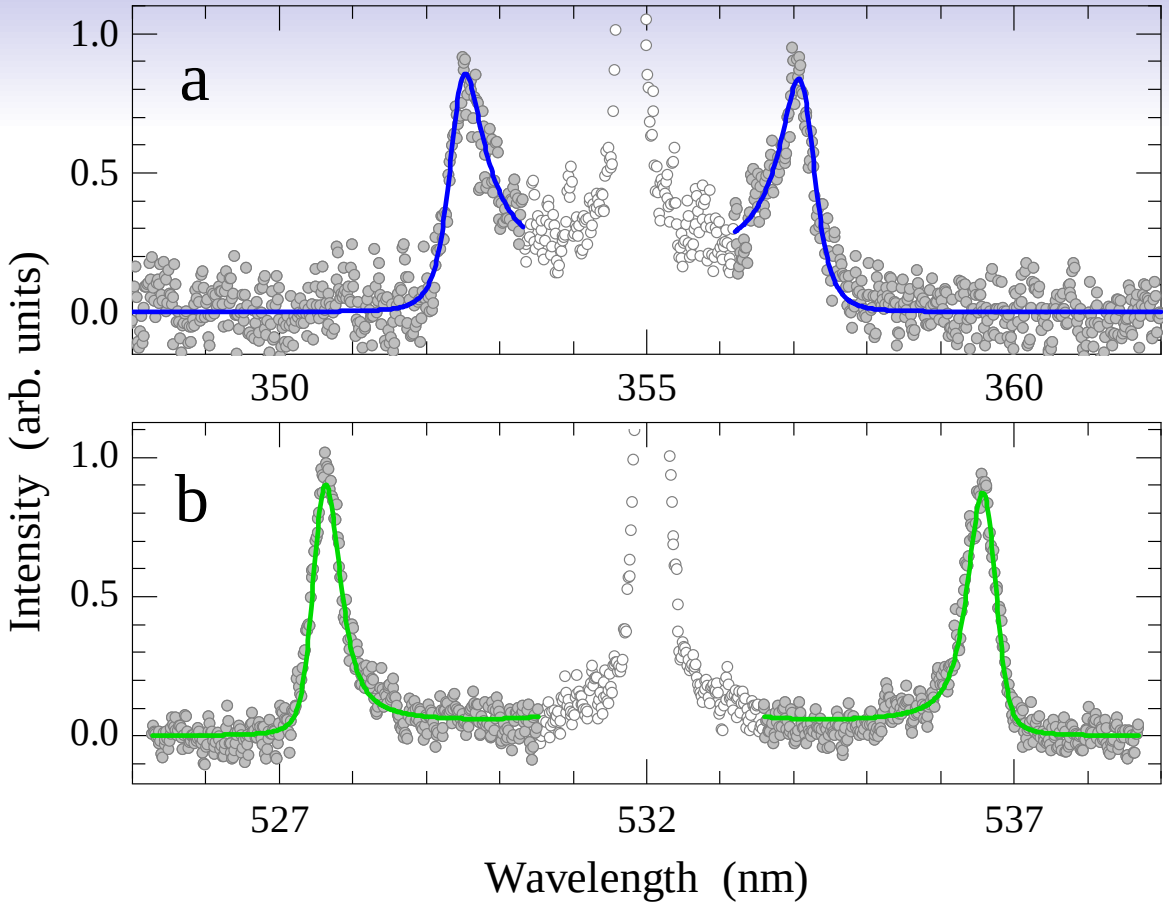

Typical TS spectra recorded on the plasma axis for two probe lasers of $355\,\mathrm{nm}$ (a) and $532\,\mathrm{nm}$ (b). Solid lines: the best fit with the electron spectral density function

$$\tilde{S}_e(\omega) \equiv [S_e(k_{355}, \omega) + S_e(k_{532}, \omega)] * f_{\mathrm{instr}}(\omega).$$

2CTS results

Delay (ns)	N_e $(10^{23}\,\mathrm{m}^{-3})$	T_e (K)	T_i (K)
60	$4.548\,^{+0.142}_{-0.052}$	$19590\,^{+330}_{-250}$	$19300\,^{+1500}_{-1400}$
180	$1.903\,^{+0.084}_{-0.060}$	$16020\,^{+270}_{-230}$	$15300\,^{+1500}_{-1400}$
350	$0.977\,^{+0.067}_{-0.078}$	$14110\,^{+500}_{-550}$	$15500\,^{+2800}_{-2800}$
500	$0.543\,^{+0.015}_{-0.028}$	$10670\,^{+300}_{-440}$	$6800\,^{+780}_{-970}$
600	$0.273\,^{+0.013}_{-0.025}$	$7680\,^{+540}_{-740}$	$5030\,^{+860}_{-1100}$
700	$0.118\,^{+0.019}_{-0.027}$	$5900\,^{+270}_{-520}$	$3200\,^{+2000}_{-2300}$

The experimentally determined values of N_e, T_e, and T_i were used in the line-shape modeling.

Comparison of theory and experiment

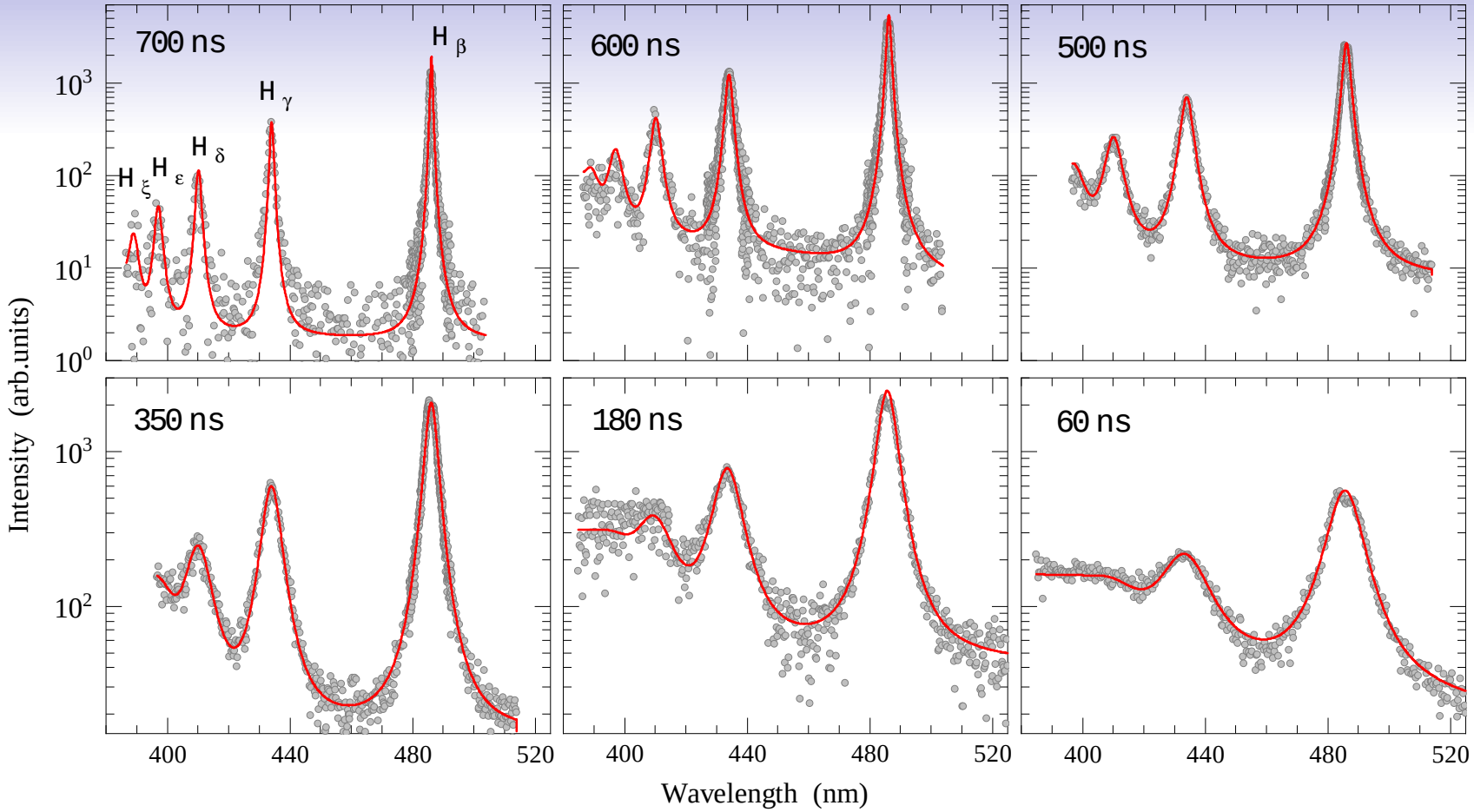

The calculations reproduce the measured spectra very well, in particular, the phenomenon of line merging below the Balmer limit seen at the higher densities.

Conclusions

- Plasma density effects manifest themselves in various atomic phenomena, including merging of the discrete and continuous spectra.
- The quasicontiguous frequency-fluctuation method (QC-FFM) was used to model entire hydrogen Balmer series – discrete lines and photorecombination continuum.
- Laser-induced hydrogen plasma was precisely diagnosed using two-color Thomson scattering (2CTS) technique, inferring N_e, T_e, and T_i.
- The theoretical spectra are found to be in good agreement with experimental ones, including higher-density data where discrete lines were observed to merge forming a continuum.
- The calculational model can be applied to spectra of hydrogen-like ions or Rydberg series of any species, providing efficient density diagnostic of laboratory and space plasmas.

Thank you for your attention!

Bibliography I


Dappen, W., Anderson, L., and Mihalas, D. (1987).
Astrophys. J., 319:195–206.


Rogers, F. J. and Iglesias, C. A. (1992).
79:507–568.


Tremblay, P. and Bergeron, P. (2009).
Astrophys. J., 696(2):1755–1770.


D'yachkov, L. G. (2016).
High Temperature, 54(1):5–10.


Lin, C., Röpke, G., Reinholz, H., and Kraeft, W.-D. (2017).
Contrib. Plasma Phys., 57(10):518–523.


Alexiou, S., Stambulchik, E., Gomez, T., and Koubiti, M. (2018).
Atoms, 6(2):13.


Koubiti, M. and Sheeba, R. R. (2019).
Atoms, 7(1):23.


Wiese, W. L., Kelleher, D. E., and Paquette, D. R. (1972).
Phys. Rev. A, 6(3):1132–1153.

Bibliography II


Morgan, W. W., Abt, H. A., and Tapscott, J. W. (1978).
Revised MK Spectral Atlas for stars earlier than the sun.
Williams Bay: Yerkes Observatory, and Tucson: Kitt Peak National Observatory.


Stambulchik, E. and Maron, Y. (2008).
J. Phys. B: At. Mol. Opt. Phys., 41(9):095703.


Talin, B., Calisti, A., Godbert, L., Stamm, R., Lee, R. W., and Klein, L. (1995).
Phys. Rev. A, 51(3):1918–1928.


Calisti, A., Mossé, C., Ferri, S., Talin, B., Rosmej, F., Bureyeva, L. A., and Lisitsa, V. S. (2010).
Phys. Rev. E, 81(1):016406.


Bureeva, L. A., Kadomtsev, M. B., Levashova, M. G., Lisitsa, V. S., Calisti, A., Talin, B., and Rosmej, F. (2010).
JETP Letters, 90(10):647–650.


Stambulchik, E. and Maron, Y. (2013).
Phys. Rev. E, 87(5):053108.


Griem, H. R. (1997).
Principles of Plasma Spectroscopy.
Cambridge University Press, Cambridge, England.

Bibliography III


Inglis, D. R. and Teller, E. (1939).
Astrophys. J., 90:439–448.


Salpeter, E. E. (1960).
Phys. Rev. A, 120(5):1528–1535.


Evans, O. E. and Katzenstein, J. (1969).
Rep. Prog. Phys., 32(1):207–271.


Sobczuk, F., Dzierżęga, K., and Stambulchik, E. (2021).
In preparation.


Dzierżęga, K., Sobczuk, F., Stambulchik, E., and Pokrzywka, B. (2021).
Phys. Rev. E, 103(6):063207.